Front. Mater. Sci. 2017, 11(1): 33–41
DOI 10.1007/s11706-017-0366-z

RESEARCH ARTICLE

Preparation of porous hollow silica spheres via a layer-by-layer process and the chromatographic performance

Xiaobing WEI[1,2], Cairong GONG (✉)[1], Xujuan CHEN[1], Guoliang FAN[1], and Xinhua XU (✉)[1]

1 School of Materials Science and Engineering, Tianjin University, Tianjin 300350, China
2 Analysis and Testing Center, Shandong University of Technology, Zibo 255000, China

ABSTRACT: Hollow silica spheres possessing excellent mechanical properties were successfully prepared through a layer-by-layer process using uniform polystyrene (PS) latex fabricated by dispersion polymerization as template. The formation of hollow SiO_2 micro-spheres, structures and properties were observed in detail by zeta potential, SEM, TEM, FTIR, TGA and nitrogen sorption porosimetry. The results indicated that the hollow spheres were uniform with particle diameter of 1.6 μm and shell thickness of 150 nm. The surface area was 511 m^2/g and the pore diameter was 8.36 nm. A new stationary phase for HPLC was obtained by using C_{18}-derivatized hollow SiO_2 micro-spheres as packing materials and the chromatographic properties were evaluated for the separation of some regular small molecules. The packed column showed low column pressure, high values of efficiency (up to about 43 000 plates/m) and appropriate asymmetry factors.

KEYWORDS: PS latex; layer-by-layer; hollow silica spheres; packing materials

Contents

Received October 26, 2016; accepted December 7, 2016

E-mails: gcr@tju.edu.cn (C.G.), xhxutju@gmail.com (X.X.)

1 Introduction

In recent years, with the rapid development of the life sciences, environmental science, and pharmaceutical and synthetic chemistry, high-performance liquid chromatography (HPLC) has become one of the most commonly used techniques for the separation and purification of multifarious compounds [1]. Chromatographic column is the core of HPLC system and the stationary phases are the basis of the development and application of HPLC.

Inorganic materials, especially, silica-based stationary phases have been widely used and developed [2–5] because of high mechanical strength and chromatography performance. Silicaceous materials have experienced the stages including from irregular to regular, from large to small, from impure to highly pure uniform silica. With the size of the packing materials progressively decreased, the column performance has been dramatically improved, meanwhile, maintaining or even booting the analytical features of HPLC [6]. However, the small particle generates every high back pressure, which requires new special hardware to handle the high-pressure conditions. The porous particles [7] and the core–shell particles [8–9] successively emerged as affective technology to improve the properties of thermal stability and high permeability. Moreover, our research group tried to get the hollow silica spheres based on a layer-by-layer technology to be used as HPLC packing.

Hollow microstructures have high specific surface areas, high capsulation capacity, and better permeation, and hence they have widespread potential applications in HPLC [10]. As we all know, the widely used strategy for synthesizing hollow structures is template method [11–13]. The templates include polymer latex spheres [14–15], carbon nanoparticles [16] and monodisperse silica spheres [17], while silica [18–20], titania [21–22], magnetite [23], silver [24], zirconia [25] have been commonly used as shell materials. Among these templates, polymers such as polystyrene (PS) are widely used core particles for its uniform spherical shape and high monodispersity. Due to the tunable chemical stability and mechanical stability, SiO_2 is considered to be an ideal alternative material that has been employed for coating on various core particles. Yuan et al. [26–27] fabricated 120 nm thiol- and vinyl-functionalized hollow SiO_2 spheres by using PS particles as hard templates, but the further applications were not reported. Deng et al. [28] developed a method to coat uniform vinyl-functionalized SiO_2 shell on negatively charged PS particles. Dong et al. [29] fabricated 6–7 layers of silica nanoparticles onto core particles using a new multilayer-by-multilayer to apply them into LC. Chen et al. [30] firstly deposited mesoporous silica on the surface of solid silica spheres to make a core/shell structure. Then by choosing the proper alkaline etching agent, the solid silica core was selectively dissolved based on the structural difference between the core and the shell. The uniformity of a chromatographic packing is important for obtaining low column pressure and low peak broadening. So more and more new type silica-based stationary phase will be used in different areas.

In the present paper, PS@SiO_2 core–shell spheres were fabricated through a layer-by-layer method using PS as the template, and the hollow silica microspheres were obtained by calcining the core–shell particles at 750°C to remove the PS template. Then C_{18}-derivatizedhollow silica microspheres were packed into the 4.6 mm × 50 mm column to examine its chromatographic performance and behavior. The formation process, structure and chromatographic properties of the hollow SiO_2 micro-spheres were studied, and the obtained C_{18}-derivatized hollow SiO_2 microspheres as packing materials had potential applications in pharmaceutical chemistry field.

2 Experimental

2.1 Materials

All the reagents were of analytical grade unless otherwise indicated. Styrene, sodium hydroxide (NaOH), alcohol (C_2H_6O), ammonia solution ($NH_3 \cdot H_2O$) were obtained from Kewei Chemical Reagent Co. Ltd. of Tianjin University (Tianjin, China), polyvinyl pyrrolidone (PVP) was from Tianjin Bodi Chemical Co. Ltd. (Tianjin, China), cetyltrimethyl ammonium bromide (CTAB) was from Tianjin Kemiou Chemical Reagent Co. Ltd. (Tianjin, China), tetraethoxysilane (TEOS) and trimethyl-chlorosilane were purchased from Sinopharm Chemical Reagent Co. Ltd., 2,2'-azobis(2-methylpropionamidine) dihydrochloride (AIBA) and 2,2'-azobisisobutyronitrile (AIBN) were supplied by Heowns Biochem Technologies LLC, and octadecyltrichlorosilane (ODTS) was obtained from Beijing Lark Technology Co. Ltd. All the reagents were analytical grade and used without further purification, and all the aqueous solutions were prepared with distilled water and styrene was used after being redistilled.

2.2 Preparation of PS latex, PS@SiO_2 and hollow SiO_2 micro-spheres

2.2.1 Synthesis of PS latex

The purchased styrene was washed by a base solution (NaOH) and distilled to remove its inhibitor. PVP, alcohol and distilled water were mixed and then the aqueous solution was put into a round bottom flask with four necks, vigorously stirred, and heated at 56°C under a nitrogen

atmosphere. The heating process was maintained for 30 min. Subsequently, the AIBA and styrene were added into the reactor. The mixing system was subsequently maintained at 56°C for 12 h under a nitrogen atmosphere. Then the reaction system was cooled to room temperature and centrifuged with water for a few times to remove impurities. Finally, the products were dried at 60°C for 8 h.

2.2.2 Synthesis of PS@SiO_2 particles and hollow SiO_2 particles

The PS@SiO_2 particles were prepared by a layer-by-layer process. In brief, the PS (0.5 g) prepared above were redispersed in a solution containing CTAB (0.1 g), distilled water (4.5 g) and ethanol (30 mL). The mixed materials were ultrasonic dispersed for 30 min to form a uniform dispersion. Then the TEOS (1.0 g) in ethanol (20 mL) were added dropwise into the dispersion with continuous stirring for 5 h at room temperature. The products were collected by centrifuge and washed with water and ethanol for three times, followed by drying at 60°C for 8 h. Finally, the purified products were calcined at 750°C for 12 h to remove both PS spheres and CTAB.

2.2.3 Surface silanization of hollow silica micro-spheres

The C_{18} surface, created by self-assembly of ODTS, has been commonly used as a surface modifier for reverse-phase chromatography stationary phases [31]. The bonding reaction was executed under the condition free of oxygen and water where ODTS was selected as silicon alkylation reagent and trimethyl chlorosilane was used as the end capping reagent. First, the hollow SiO_2 spheres were immersed in the hydrochloric acid (0.1 mol/L) for 12 h, washed sequentially with distilled water until no chloridion detected, dried in vacuum at 60°C for 1 h to get more active hydroxyl silicon. The hollow SiO_2 spheres (2 g) were added in a flask with three necks (100 mL), then dried in vacuum for 1 h until the water vapor disappeared. Under the condition of toluene reflux at 110°C, the derivative reaction of the hollow SiO_2 spheres, ODTS (2 mL) and triethylamine catalyst (0.5 mL) was processed under N_2 for 24 h. After stirring at ambient temperature, trimethyl chlorosilane was added to handle the seals of the product for cover the unreacted silicon hydroxyl groups, the reaction was refluxed for 24 h under N_2. Finally, the reaction generated the products containing $Si-O-Si$ bonded stationary phase which were named as C_{18}-SiO_2.

2.3 Characterization of materials

Scanning electron microscopy (SEM; Sirion200, FEI) and transmission electron microscopy (TEM; JEM-1011, FEI) were used to study the morphology and the structure of the composite. The zeta potentials of the PS latex dispersed into the deionized water were tested on the Zeta-Potential-Analyzer of BL-90Plus. The nitrogen adsorption–desorption isotherms were measured by N_2 adsorption at -196°C using NOVA 2000 gas sorption analyzer, and the pore size distribution (PSD) of samples were calculated using the Barrett–Joyner–Halenda (BJH) algorithm. Specific surface areas were calculated by the Brunaure–Emmert–Teller (BET) method. Fourier transform infrared spectroscopy (FTIR; Nicolet 5700, Thermo Electron Corporation) spectra of samples in KBr pellets were measured with a Bio-Rad FTS6000 spectrometer. Thermogravimetric analysis (TGA; Pyris Diamond, Perkin-Elmer, USA) was performed on a instrument in the range of 30°C–1000°C under 100 mL/min air flux with a heating rate of 10°C/min.

Wet packing column method was adopted to obtain the packing column (50 mm × 4.6 mm) on stationary phase of C_{18}-derivatized hollow SiO_2 spheres. Three compounds including benzene, benzyl alcohol and benzaldehyde were selected to value the performance of column. All chromatographic separations were performed on an Agilent 1100 HPLC system equipped with a quaternary pump and UV-vis (254 nm) detector. The mobile phase consisted of acetonitrile and water was used as gradient elution for separation with reverse-phase liquid chromatography, and injection volume of 10 μL, flow rates of 1.0 mL/min at 25°C.

3 Results and discussion

3.1 Characterization of PS latex

The kind of initiator in the reaction medium has a pronounced influence on the surface charge and particle size of the PS latex. The zeta potential of the PS latex initiated by AIBN and AIBA is summarized in the Table 1. It is easy to find that the surface potential of PS latex initiated by AIBA is positive in neutral or alkaline condition. On the contrary, the surface potential of the PS initiated by AIBN is negative. It can also be found that the potential of the silica particle is negative, so the PS initiated by AIBA is the better candidate to fabricate the PS@SiO_2 particles. The SEM image of the PS latex initiated by AIBA

is shown in Fig. 1(a). It can be seen that the particles fabricated by dispersion polymerization utilizing AIBA as initiator are mono-disperse with an average size of 1.5 μm, and the positive particles are suitable as templates for silica coating without any other treatment.

Table 1 The zeta potential of the PS initiated by different initiators and SiO_2 colloids

Sample	pH	Surface potential /mV
PS (AIBA)	7	4.23
PS (AIBA)	9	5.25
PS (AIBN)	7	−6.50
PS (AIBN)	9	−4.02
SiO_2	7	−26.33

3.2 Characterization of PS@SiO_2 and hollow SiO_2 micro-spheres

The SEM and TEM images of the PS latex, PS@SiO_2 and hollow SiO_2 micro-spheres are shown in Fig. 1. The particle size of the PS latex was estimated to be about 1.5 μm and the shape was uniform from Figs. 1(a) and 1(d). Figure 1(b) gives the SEM image of PS@SiO_2 micro-spheres. It can be inferred that SiO_2 has been successfully coated on the surface of PS spheres eventually. The corresponding TEM image shows PS@SiO_2 core/shell particles (shown in Fig. 1(e)) possessing a core with an average diameter of 1.5 μm and a uniform shell with a coating thickness of about 150 nm. After calcined at 750°C, hollow SiO_2 was obtained and the corresponding SEM image is shown in Fig. 1(c). The interior space of the hollow SiO_2 is clearly revealed in the SEM image from some broken silica spheres from Fig. 1(c). Figure 1(f) gives the typical TEM image of the hollow silica colloids and each sphere structure has a uniform shell.

The particle size distribution of the hollow SiO_2 micro-spheres is also detected by zeta potential analyzer. It can be seen from Fig. 2 that the particle size is centered at 1.6 μm, which is in good harmony with SEM and TEM results, and the packing materials with uniform size is optimal for stationary phase.

Figure 3 shows the nitrogen adsorption and desorption isotherms and pore size distribution of PS@SiO_2 and hollow SiO_2 micro-spheres. As shown in Fig. 3(a), the PS@SiO_2 spheres had typical type IV isotherms, which indicated that the materials were of uniform pore size and regular shape, and the pore structure was approximately cylindrical structure, meanwhile, the phenomenon of capillary condensation emerged in the process of adsorption. As the inset in Fig. 3(a) shown, the pore size distribution mainly centered on 8.36 nm, which had a narrow pore size distribution. After the removal of PS, hollow SiO_2 spheres kept the pore size of PS@SiO_2, as shown in Fig. 3(b). The hollow silica microspheres obtained a specific surface area of 511 m^2/g by using the BET method, and the surface area of the materials was higher compared with Ref. [32] reported 474 m^2/g. It was an important foundation for liquid chromatography packing materials, because high specific surface area helped increase the flow of time in the column, and thus could achieve better separation effect.

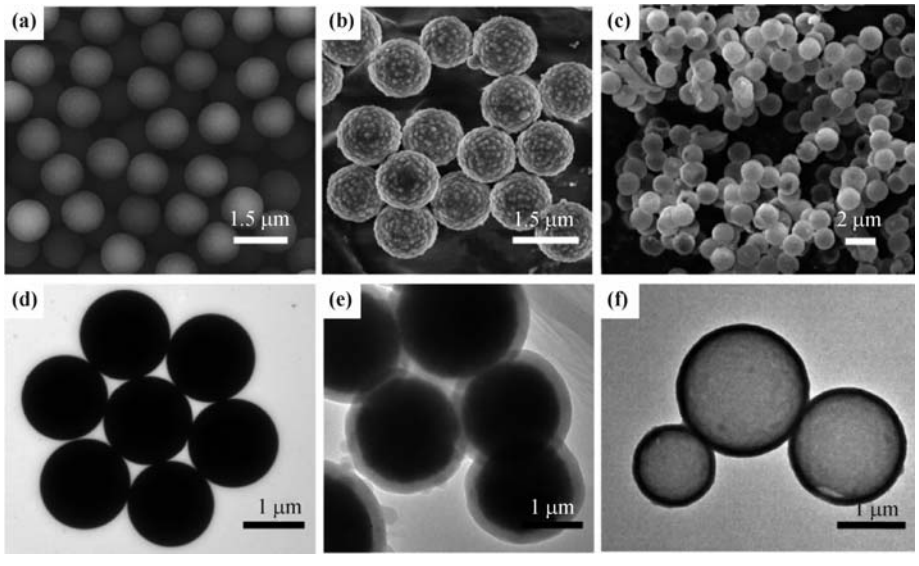

Fig. 1 SEM images of **(a)** PS latex, **(b)** PS@SiO_2 and **(c)** hollow SiO_2 micro-spheres. TEM images of **(d)** PS latex, **(e)** PS@SiO_2 and **(f)** hollow SiO_2 micro-spheres.

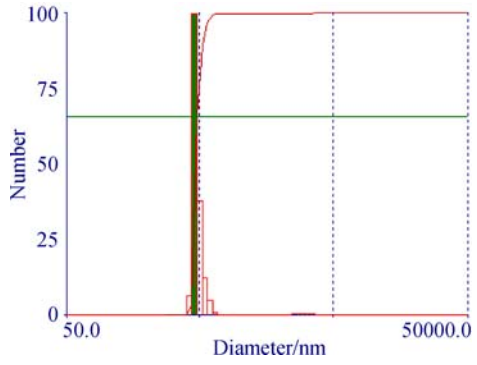

Fig. 2 The particle size distribution of hollow SiO_2 micro-spheres.

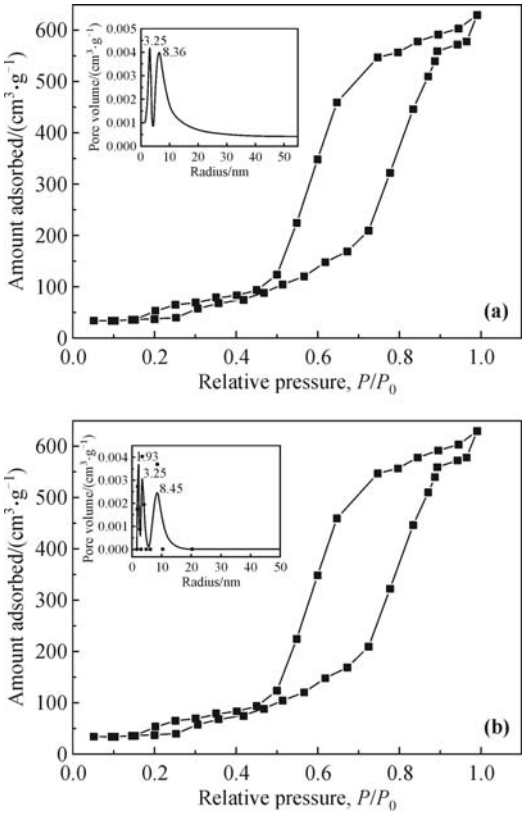

Fig. 3 Nitrogen adsorption–desorption isotherms and insert image is corresponding pore size distribution of **(a)** PS@SiO_2 and **(b)** hollow SiO_2 spheres.

3.3 Formation of hollow SiO_2 micro-spheres, structures and properties

Figure 4(a) shows FTIR spectra of SiO_2, PS@SiO_2 and PS. In the IR spectrum of SiO_2 (Curve I in Fig. 4(a)), the peak at 466 cm^{-1} is due to the bending vibration of Si–O–Si, and peaks at 798 and 1079 cm^{-1} are ascribed to the symmetric and the asymmetric stretching vibrations of Si–O–Si, respectively. Those three are the characteristic peaks of SiO_2 [33]. Peaks at around 1638 and 3473 cm^{-1} represent respectively the bending vibration and the stretching vibration of –OH of H_2O adsorbed on the surface of the sample or into the pores of SiO_2 [34]. In the spectra of PS latex (Curve III in Fig. 4(a)), the peak at 3025 cm^{-1} corresponds to the stretching vibration of C–H in the benzene ring [35], peaks at 2921 and 2841 cm^{-1} belong to the symmetric and the asymmetric stretching vibrations of saturated C–H, the four small peaks between 1600–2100 cm^{-1} can be attributed to the bending vibration overtones of =C–H in the mono-substituted benzene, and the three peaks at 1600, 1490 and 1450 cm^{-1} are mainly ascribed to the vibration of the benzene ring framework, and meanwhile, the peaks at 775 and 698 cm^{-1} are the characteristic peaks of single substituted benzene [36]. In the spectrum of the PS@SiO_2 composite (Curve II in Fig. 4(a)), peaks assigned to PS at 698 and 775 cm^{-1} etc., and the peaks assigned to SiO_2 at 466, 798 and 1079 cm^{-1} still exist, and no significant new peak is observed, indicating that the PS@SiO_2 composite is just a physical interaction or electrostatic interaction between PS and SiO_2, producing no chemical bond. The results of FTIR show that the PS@SiO_2 particles are successfully fabricated.

Figure 4(b) shows FTIR spectra of SiO_2 and C_{18}-SiO_2. Comparing with that of SiO_2 (Curve I in Fig. 4(b)), the IR spectrum of C_{18}-SiO_2 (Curve II in Fig. 4(b)) appears new characteristic peaks. The peaks at 2923 and 2854 cm^{-1} correspond to the stretching vibration of saturated C–H, and the absorption peak at 1465 cm^{-1} belongs to the bending vibration of $-CH_2$ and $-CH_3$, all of which demonstrate that the functional group of $-C_{18}$ has successfully bonded on the surface of SiO_2.

Figure 5 shows TG and DSC curves of PS@SiO_2. It can be seen that the first weight loss begins at 300°C in the curve of TG, and it is easy to find that the biggest weight loss rate is approximately at 330°C in the curve of DTG. But when the temperature reaches 420°C, the mass of the materials mainly keeps steady. The second weight loss occurs at 500°C, and ends at 600°C along with the biggest weight loss at 570°C. Corresponding to the TG result, the curve of DSC shows that there is a big endothermic peak at 330°C mainly because of the decomposition of PS, which is in accordance with the first weight loss in the curve of TG. The second endothermic peak appears at about 570°C as a result of the carbonized decomposition of CTAB, which is one of the cationic surface active agents, and at the same time there is a weight loss in the TG. In conclusion,

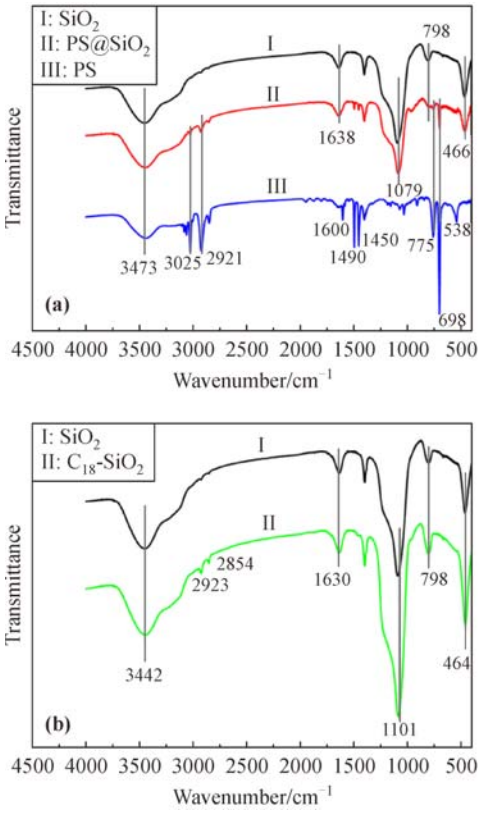

Fig. 4 FTIR spectra: **(a)** including SiO_2 (I), PS@SiO_2 (II) and PS (III); **(b)** including SiO_2 (I) and C_{18}-SiO_2 (II).

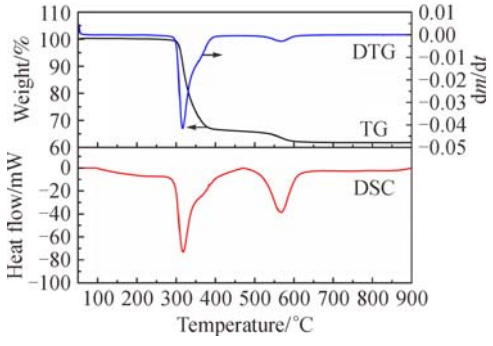

Fig. 5 DTG, TG and DSC curves of the PS@SiO_2.

only when the calcination temperature is up to 600°C can PS and organic purities used in the experiment be removed completely.

For chromatographic applications, the mechanical strength of the particles is critically important. However, the porous shells prepared by the layer-by-layer method are assembled loosely and packed silica nanoparticles are held together by weak electrostatic attractions and hydrogen bonding. These forces are unlikely to impart sufficient mechanical stability to produce robust shells [37–38]. To enhance the mechanical strength of porous silica films, low temperature methods such as hydrothermal treatment [37] and atomic layer deposition [39] have recently been developed. In this work, we explored high temperature treatment as a method to enhance the mechanical strength of hollow SiO_2 spheres. In order to test the mechanical strength of our materials, we prepared KBr pellets similar to those used for recording IR spectra, using different final pressures (550°C, 100 psi (1 psi = 6.895×10^3 Pa); 650°C, 250 psi; 750°C, 100 psi; 750°C, 250 psi) to form the pellets and then characterized by SEM. As shown in Fig. 6, after the pressure, the hollow silica spheres obtained at 550°C and 650°C crushed, while that obtained at 750°C kept the hollow sphere structure. It can be inferred that the mechanical strength of the hollow SiO_2 spheres increased with the increase of the sintering temperature, which might come from the increase of the density of the hollow sphere. Because the layers of hollow spheres prepared are generated by self-assembly, the higher sintering temperature will make the adhesion between pellets reduced. Therefore, the sintering temperature should be appropriate, thus the temperature of 750°C is suitable. It can also conclude that the packing materials can bear a pressure as high as 250 psi. It is worth mentioning that the column pressure of the packing column using the hollow spheres as packing materials is only 60 psi which will deal with in the chromatographic performance section.

Selecting the wet packing column method to obtain the packing column (50 mm × 4.6 mm) on stationary phase of the hollow SiO_2 spheres bonded octadecylsilane. The

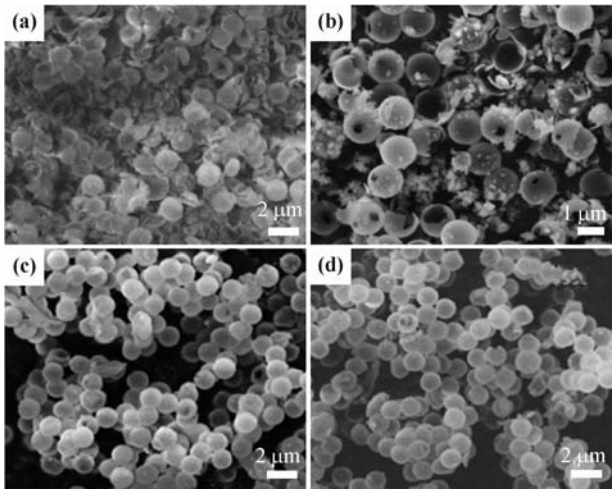

Fig. 6 SEM images of hollow silica spheres treated at different temperature that are subjected to high compressive pressure: **(a)** 550°C, 100 psi; **(b)** 650°C, 250 psi; **(c)** 750°C, 100 psi; **(d)** 750°C, 250 psi.

column pressure (ΔP) and relevant permeability (κ) of different flow rates would be tested by HPLC (Agilent 1100). Equation (1) can explain the relationship of ΔP, κ and F:

$$\kappa = \frac{F\eta L}{r^2 \pi \Delta P} \tag{1}$$

where F is flow rate, L is the length of column, η is viscosity of moving phase, and r is the radius of column.

Figure 7 shows that the column pressure drop, permeability and flow rate are fit for the linear relation. The column pressure is low at the ordinary flow rate. Normal pore size and good permeability make the elution well to separate the sample quickly. When the flow rate is 1 mL/min, the column pressure is only 4 atm (1 atm = 1.013×10^5 Pa) less than the regular LC column pressure which is often 50–100 atm empirically. This demonstrates that the home-made packing materials own high resistance to pressure and improving the column property.

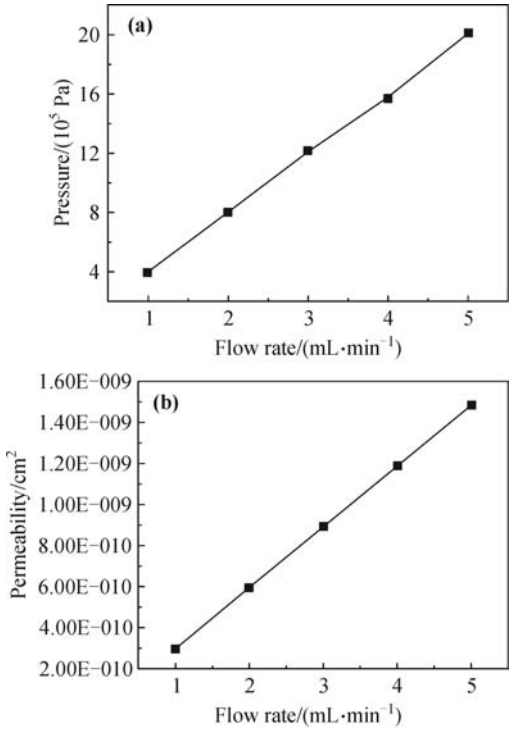

Fig. 7 **(a)** The relationship between column pressure and flow rate. **(b)** The relationship between permeability and flow rate.

Herein, the chromatographic performance of hollow silica spheres as stationary of column for the separation of small molecules was tested. As presented in Fig. 8, three kinds of compounds benzene, benzyl alcohol and benzaldehyde were completely separated on the home-made column. Peak identifications in order: benzene (1.980 min), benzyl alcohol (5.193 min) and benzaldehyde (13.858 min). In spite of using a short column a suitable separation with good resolution and peak symmetries were obtained where the average of resolution is more than 4.00 and asymmetry factors are about 0.98–1.10. Moreover, number of theoretical plates is achieved about 43 000 N/m and the column pressure is 60 psi which is much lower than that of UPLC.

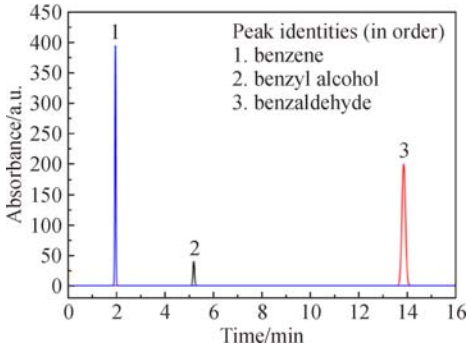

Fig. 8 Chromatogram for the separation of three compounds, benzene, benzyl alcohol and benzaldehyde on stationary phase home-made hollow silica spheres.

4 Conclusions

Hollow SiO_2 micro-spheres were fabricated through a layer-by-layer process using PS latex as the template. The diameter was about 1.6 μm and the size distribution was narrow and the thickness of the shell was about 150 nm. The packing column using C_{18}-derivatized hollow SiO_2 micro-spheres as packing materials has low column pressure, good mechanical strength and chromatography performance. Such packing materials with high mechanical strength and efficient separation as the LC stationary phase would be promising in the fields of pharmaceutical analytical chemistry. The studies to improve the durability for long time use and reproducibility of separation of the packing column are in the process.

Declaration of conflicting interests The authors declare that there is no conflict of interest.

Acknowledgements This project was supported by the National Natural Science Foundation of China (Grant No. 51406109).

References

[1] Wang L, Wei W, Xia Z, et al. Recent advances in materials for

stationary phases of mixed-mode high-performance liquid chromatography. Trends in Analytical Chemistry, 2016, 80: 495–506

[2] Unger K K, Skudas R, Schulte M M. Particle packed columns and monolithic columns in high-performance liquid chromatography — comparison and critical appraisal. Journal of Chromatography A, 2008, 1184(1–2): 393–415

[3] Zhao B B, Zhang Y, Tang T, et al. Silica based stationary phases for high performance liquid chromatography. Progress in Chemistry, 2012, 24(1): 122–130 (in Chinese)

[4] Zhao L, Yang L, Wang Q. Silica-based polypeptide-monolithic stationary phase for hydrophilic chromatography and chiral separation. Journal of Chromatography A, 2016, 1446: 125–133

[5] Qiu H, Liang X, Sun M, et al. Development of silica-based stationary phases for high-performance liquid chromatography. Analytical and Bioanalytical Chemistry, 2011, 399(10): 3307–3322

[6] Miyabe K. New moment equations for chromatography using various stationary phases of different structural characteristics. Analytical Chemistry, 2007, 79(19): 7457–7472

[7] Ali I, Al-Othman Z A, Al-Za'abi M. Superficially porous particles columns for super fast HPLC separations. Biomedical Chromatography, 2012, 26(8): 1001–1008

[8] Abrahim A, Al-Sayah M, Skrdla P, et al. Practical comparison of 2.7 μm fused-core silica particles and porous sub-2 μm particles for fast separations in pharmaceutical process development. Journal of Pharmaceutical and Biomedical Analysis, 2010, 51 (1): 131–137

[9] Dong H, Brennan J D. Rapid fabrication of core–shell silica particles using a multilayer-by-multilayer approach. Chemical Communications, 2011, 47(4): 1207–1209

[10] Wang Y, Su X, Ding P, et al. Shape-controlled synthesis of hollow silica colloids. Langmuir, 2013, 29(37): 11575–11581

[11] Caruso F, Caruso R A, Möhwald H. Nanoengineering of inorganic and hybrid hollow spheres by colloidal templating. Science, 1998, 282(5391): 1111–1114

[12] Liu J, Liu F, Gao K, et al. Recent developments in the chemical synthesis of inorganic porous capsules. Journal of Materials Chemistry, 2009, 19(34): 6073–6084

[13] Dash B C, Réthoré G, Monaghan M, et al. The influence of size and charge of chitosan/polyglutamic acid hollow spheres on cellular internalization, viability and blood compatibility. Biomaterials, 2010, 31(32): 8188–8197

[14] Zeng H, Xu X, Bando Y, et al. Template deformation-tailored ZnO nanorod/nanowire arrays: full growth control and optimization of field-emission. Advanced Functional Materials, 2009, 19(19): 3165–3172

[15] Zhao B, Collinson M M. Hollow silica capsules with well-defined asymmetric windows in the shell. Langmuir, 2012, 28(19): 7492–7497

[16] Dong Z, Lai X, Halpert J E, et al. Accurate control of multishelled ZnO hollow microspheres for dye-sensitized solar cells with high efficiency. Advanced Materials, 2012, 24(8): 1046–1049

[17] Strandwitz N C, Shaner S, Stucky G D. Compositional tunability and high temperature stability of ceria–zirconia hollow spheres. Journal of Materials Chemistry, 2011, 21(29): 10672–10675

[18] Zou H, Wu S, Shen J. Polymer/silica nanocomposites: preparation, characterization, properties, and applications. Chemical Reviews, 2008, 108(9): 3893–3957

[19] Hu H, Zhou H, Liang J, et al. Facile synthesis of amino-functionalized hollow silica microspheres and their potential application for ultrasound imaging. Journal of Colloid and Interface Science, 2011, 358(2): 392–398

[20] Hebalkar N Y, Acharya S, Rao T N. Preparation of bi-functional silica particles for antibacterial and self cleaning surfaces. Journal of Colloid and Interface Science, 2011, 364(1): 24–30

[21] Karabacak R B, Erdem M, Yurdakal S, et al. Facile two-step preparation of polystyrene/anatase TiO_2 core/shell colloidal particles and their potential use as an oxidation photocatalyst. Materials Chemistry and Physics, 2014, 144(3): 498–504

[22] Demirörs A F, van Blaaderen A, Imhof A, et al. Synthesis of eccentric titania–silica core–shell and composite particles. Chemistry of Materials, 2009, 21(6): 979–984

[23] Wen H Y, Gao G, Han Z R, et al. Magnetite-coated polystyrene hybrid microspheres prepared by miniemulsion polymerization. Polymer International, 2008, 57(4): 584–591

[24] Nithyadevi D, Kumar P S, Mangalaraj D, et al. Improved microbial growth inhibition activity of bio-surfactant induced Ag–TiO_2 core shell nanoparticles. Applied Surface Science, 2015, 327: 504–516

[25] Stephenson R C, Partch R E. Metal oxide and metal carbide thin film coatings on large spherical particles. MRS Online Proceedings Library, 1996, 458: 435

[26] Yuan J, Wan D, Yang Z. A facile method for the fabrication of thiol-functionalized hollow silica spheres. The Journal of Physical Chemistry C, 2008, 112(44): 17156–17160

[27] Pu H, Zhang X, Yuan J, et al. A facile method for the fabrication of vinyl functionalized hollow silica spheres. Journal of Colloid and Interface Science, 2009, 331(2): 389–393

[28] Deng T S, Marlow F. Synthesis of monodisperse polystyrene@-vinyl-SiO_2 core–shell particles and hollow SiO_2 spheres. Chemistry of Materials, 2012, 24(3): 536–542

[29] Dong H, Brennan J D. Tailoring the properties of sub-3 μm silica core–shell particles prepared by a multilayer-by-multilayer process. Journal of Colloid and Interface Science, 2015, 437: 50–57

[30] Chen Y, Chen H, Guo L, et al. Hollow/rattle-type mesoporous

nanostructures by a structural difference-based selective etching strategy. ACS Nano, 2010, 4(1): 529–539

[31] Huang T T, Geng T, Akin D, et al. Micro-assembly of functionalized particulate monolayer on C_{18}-derivatized SiO_2 surfaces. Biotechnology and Bioengineering, 2003, 83(4): 416–427

[32] Sun S, Zhang X, Han Q, et al. Preparation and retention mechanism exploration of mesostructured cellular foam silica as stationary phase for high performance liquid chromatography. Talanta, 2016, 149: 187–193

[33] Wang R, Tang J, Liu J, et al. Preparation of Ag@SiO_2 dispersion in different solvents and investigation of its optical properties. Journal of Dispersion Science and Technology, 2011, 32(4): 532–537

[34] Wang W, Gu B, Liang L. Effect of surfactants on the formation, morphology, and surface property of synthesized SiO_2 nanoparticles. Journal of Dispersion Science and Technology, 2005, 25(5): 593–601

[35] Iyer R, Suin S, Shrivastava N K, et al. Compatibilization mechanism of nanoclay in immiscible PS/PMMA blend using unmodified nanoclay. Polymer-Plastics Technology and Engineering, 2013, 52(5): 514–524

[36] Liu P. Facile preparation of monodispersed core/shell zinc oxide@polystyrene (ZnO@PS) nanoparticles via soapless seeded microemulsion polymerization. Colloids and Surfaces A: Physicochemical and Engineering Aspects, 2006, 291(1–3): 155–161

[37] Gemici Z, Shimomura H, Cohen R E, et al. Hydrothermal treatment of nanoparticle thin films for enhanced mechanical durability. Langmuir, 2008, 24(5): 2168–2177

[38] Blue L E, Jorgenson J W. 1.1 μm superficially porous particles for liquid chromatography. Part I: synthesis and particle structure characterization. Journal of Chromatography A, 2011, 1218(44): 7989–7995

[39] Dafinone M I, Feng G, Brugarolas T, et al. Mechanical reinforcement of nanoparticle thin films using atomic layer deposition. ACS Nano, 2011, 5(6): 5078–5087